Preprint
UCRL-JC-139675

The AERI/GOES Retrievals versus Radiosondes for Driving SCMs

S.C. Xie, R.T. Cederwall, J.J. Yio, W.F. Feltz, D.D. Turner and M.H. Zhang

This article was submitted to
10th Atmospheric Radiation Measurement (ARM) Science Team Meeting
San Antonio, TX
March 13-17,2000

U.S. Department of Energy

Lawrence
Livermore
National
Laboratory

July 13, 2000

The AERI/GOES Retrievals versus Radiosondes for Driving SCMs

S. C. Xie, R. T. Cederwall, and J. J. Yio
Lawrence Livermore National laboratory
Livermore, California

W. F. Feltz
University of Wisconsin-Madison
Space Science and Engineering Center
Madison, Wisconsin

D. D. Turner
Pacific Northwest National Laboratory
Richland, Washington

M. H. Zhang
State University of New York at Stony Brook
Stony Brook, New York

Introduction

Single-Column Models (SCMs) require observations to provide suitable initial and boundary conditions. To meet this need, the Atmospheric Radiation Measurement (ARM) program conducts Intensive Observing Periods (IOPs) to provide 3-hourly radiosondes and other observations. However, such high-frequency sonde launches can be expensive. Therefore, the ARM program can only support a couple IOPs each year with each one lasting 2 - 4 weeks. In order to reduce the need for high-frequency sonde launches and to potentially expand the periods available for SCM simulations, we have conducted a study using the Atmospheric Emitted Radiance Interferometer (AERI) and Geostationary Operational Environmental Satellite (GOES) temperature and moisture retrievals, instead of radiosondes, in the ARM variational analysis system (Zhang and Lin, 1997; Zhang et al., 2000) to derive the large-scale forcing terms for driving SCMs during the March 1999 IOP. We have compared the large-scale forcing and associated SCM simulations for various combinations of data sources used in the variational analysis.

AERI/GOES Retrievals

The retrieved temperature and water vapor profiles are obtained from the combination of the AERI and GOES retrievals. There are five AERI instruments located near the Southern Great Plain (SGP) Central Facility and the four SGP Boundary Facilities (see Fig. 1) to measure downwelling atmospheric radiance from 3.3 - 18.2 μm every eight minutes. The temperature and water vapor profiles were retrieved from the radiance spectra through a physical retrieval algorithm proposed by Smith et al. (1999). Due to

the strength of the IR signal at the surface from emission within the lower atmosphere, the weighting functions become quite broad at 2.5-3.0 km and thus the retrievals using only AERI data are limited to this altitude. During precipitation events, profiles are not retrieved because a hatch is closed to protect the instrument's foreoptics. Above the upper planetary boundary layer (PBL), the temperature and water vapor profiles were retrieved hourly from the GOES sounder brightness temperature data by using a physical retrieval algorithm (Menzel et al. 1998, Ma et al. 1999). In order for the GOES to retrieve temperature and water vapor profiles, the sky conditions must be clear or broken. The first guess used to produce the GOES physical retrieval of temperature and moisture is derived from the initial analysis of the National Weather Service ETA model. Since GOES does very little to influence the temperature profile over land and primarily modifies the moisture structure, the AERI/GOES temperature profile above 700 mb is primarily from the ETA model. Detailed discussion of the data can be found in Turner et al. (2000), Feltz et al. (1998), and Smith et al. (1999).

AERI/GOES retrieval strategies used in the variational analysis

The objective analysis method used in this study is the constrained variational analysis developed by Zhang and Lin (1997). In the scheme, the atmospheric state variables are forced to conserve the column-integrated mass, moisture, dry static energy, and momentum. Table 1 lists the experiments conducted in this study. Exp. S is the standard run. It uses temperature (T) and moisture (q) profiles from radiosondes and horizontal wind fields (u, v) from radiosondes merged with wind profiler data. The Rapid Update Cycle (RUC) model data is used as the background for the variational analysis. Note that the moisture profile used in this study has been scaled to the Microwave Radiometer (MWR) water vapor measurement in order to reduce the dry bias found in regular sounding measurement. Exp. A is the same as Exp. S except using the AERI/GOES retrieved temperature and moisture profiles. Since we assume that there are no sounding data available in this case, the horizontal wind fields are only from wind profiler data in Exp. A. Exp. B is the same as Exp. A except using the RUC horizontal wind data. We conducted this experiment to study how the variational analysis is sensitive to the wind fields. As a reference, Exp. C shows results from the variational analysis using the RUC data only. The constraints used in the variational analysis are the same for all experiments. These constraints include surface precipitation, latent and sensible heat fluxes, and net radiative fluxes at surface and top of atmosphere (TOA). Detailed description of these constraints can be found in Zhang and Lin (1997). The locations for these data sources are shown in Fig. 1.

Variational Analysis Results

Fig. 2 shows the missing retrievals and sounding data for the SGP central facility and the four SGP boundary facilities. The numbers in the color bar represent the number of stations. It is seen that the AERI/GOES retrievals are missing most of the stations during precipitation events. Therefore, for the purpose of this paper, we ran the variational analysis only for data over the five non-precipitation days from 3/2/99 – 3/6/99. Note

that the sounding data were missing from 3/11/99 – 3/12/99 because a large snow storm temporarily halted the SCM IOP.

(1) Atmospheric state variables

Figs. 3 and 4 show temperature and moisture differences from Exp. S for Exps. A, B, and C, respectively. The temperature differences between radiosondes and retrievals (upper two panels) are large in the upper troposphere while the differences are relatively small (< 1 K) in the PBL. Note that the temperature profile in the upper troposphere for Exp. A is primarily from the ETA model, indicating that a more accurate model is required to provide a better estimate of the atmospheric state to the retrievals. For the moisture field, the AREI/GOES retrievals are slightly more moist than the sondes (< 1 g/kg) in the lower troposphere. The figures also show differences in both the temperature and moisture fields between the RUC and the sondes are relatively small compared to the retrievals. This implies that the RUC model could provide a better first guess than the ETA model for the retrievals.

Figs. 5 and 6 show differences in the horizontal wind fields from Exp. S for Exps. A, B, and C, respectively. Large biases from the sondes are shown in the upper troposphere for both the wind profiler data (used in Exp. A) and the RUC model data (used in Exps. B and C). Note that the soundings represent point measurements and the profilers measure wind over a 500 m thick layer. Therefore, the two are not expected to completely agree with each other. However, the large discrepancies among different data sources could cause problems in deriving the large-scale advective tendency and vertical motion.

(2) Derived fields

The vertical velocity and the large-scale advective tendencies of temperature and moisture shown in Figs. 7, 8, and 9 are derived from the objective analysis without using any constraints. Large differences are seen among these experiments in the figures. However, it is encouraging to see that these derived large-scale forcing terms agree well with those derived from sounding data when the constrained variational analysis is used (Figs. 10, 11, and 12) although differences are large in the original upper air data (e.g. wind fields) as discussed above. Exps. A, B, and C successfully capture the main events shown in Exp. S. This is consistent with Zhang et al. (2000), in which they found that the variational constraining processing significantly reduced the sensitivity of the final data products. In the figures, the forcings in Exp. A are generally weaker than those in Exp. S. A better agreement with Exp. S is obtained when the RUC wind fields replace the wind profiler data (Exp. B). The forcing fields derived from Exp. B are closer to those in Exp. C than those in Exp. A, indicating the importance of wind fields in the objective analysis.

SCM Results

Sensitivity of SCM simulations to the forcing data derived from the constrained variational analysis is investigated in the study. The CCM3 SCM with a modified

convection triggering condition (Xie and Zhang, 2000) is used in the experiments. Figs. 12 and 13 display the temperature and moisture errors produced by the SCM using the forcing derived from Exps. S, A, B, and C. The temperature and moisture profiles from Exp. S are used as the observed values. Generally, errors produced by these experiments are very similar. All experiments produce cold biases in the temperature field and moist biases in the moisture field. The SCM is not sensitive to the small difference in the forcing data. The principal behavior of the SCM can be captured using these forcing data.

Summary

In this study, we conducted several experiments to evaluate the use of AERI/GOES retrievals instead of radiosondes in the variational analysis. This study shows that the AERI/GOES retrievals can provide relatively accurate temperature and moisture profiles within the boundary layer. However, the temperatures above the PBL show large biases. A work to improve the upper level temperature retrievals by using the RUC temperature profile as the first guess in the GOES physical retrievals is ongoing.

The large difference in winds between radiosondes and wind profiler data presents the largest problem in using remotely sensed data when radiosondes are not available. The RUC model also shows large error in the wind fields. These differences can significantly affect the derived large-scale forcing terms if no constraints are used in the objective analysis. However, it is encouraging to see that the constrained variational analysis can largely desensitize the derived large-scale forcings to differences in the original upper air data. SCM tests also show that main behaviors of the SCM can be captured using the large-scale forcing derived from the variational analysis using the AERI/GOES retrievals, compared to the forcing derived from radiosondes.

This work was performed under the auspices of the U.S. Dept. of Energy at UC/LLNL under contract no. W-7405-Eng-48.

References

Feltz, W. F., W. L. Smith, R. O. Knuteson, H. E. Revercomb, H. M. Woolf, and H. B. Howell, 1998: Meteorological applications of temperature and water vapor retrievals from the ground-based atmospheric emitted radiance interferometer (AERI). *J. Appl. Meteor.*, **37**, 857-875.

Ma, X. L., T. J. Schmit, and W. L. Smith, 1999: A nonlinear physical retrieval algorithm—its application to the GOES-8/9 sounder. *J. Appl. Meteor.*, **38**, 501-513.

Menzel, W. P., F. C. Holt, T. J. Schmit, R. M. Aune, A. J. Schreiner, G. S. Wade, and D. G. Gray, 1998: Application of GOES-8/9 soundings to weather forecasting and nowcasting. *Bull. Amer. Meteor. Soc.*, **79**, 2059-2077.

Smith, W. L., W. F. Feltz, R. O. Knuteson, H. E. Revercomb, H. B. Howell, and H. M. Woolf, 1999: The retrieval of planetary boundary layer structure using ground-based infrared spectral radiance measurements. *J. Atmos. Oceanic Technol*., **16**, 323-333.

Turner, D. D., W. F. Feltz, and R. A. Ferrare, 2000: Continuous water profiles from operational active and passive remote sensors. *Bull. Amer. Meteor. Soc*., **81**, 1301-1317.

Xie, S. C., and M. H. Zhang, 2000: Impact of the convection triggering function on the Single-Column Model simulations. *J. Geophys. Res*., **105**, 14983-14996.

Zhang, M. H., and J. L. Lin, 1997: Constrained variational analysis of sounding data bases on column-integrated budgets of mass, heat, moisture, and momentum: Approach and application to ARM measurements. *J. Atmos. Sci*., **54**, 1503-1524.

Zhang, M. H., J. L. Lin, R. T. Cederwall, J. J. Yio, and S. C. Xie, 2000: Objective analysis of ARM IOP data: method, features, and sensitivity. Submitted to *Mon. Wea. Rev*.

Captions

Table 1. Summary of experiments.

Fig. 1 Locations: Radiosondes (×), AERI (_), NOAA wind profilers (Δ), RUC model grid (+), and final analysis grid (*).

Fig. 2 Missing retrieval and sounding data among the SGP Central Facility and the four SGP Boundary Facilities.

Fig. 3 Temperature differences from Exp. S for Exps. A, B, and C.

Fig. 4 Moisture differences from Exp. S for Exps. A, B, and C.

Fig. 5 Horizontal wind (u) differences from Exp. S for Exps. A, B, and C.

Fig. 6 Horizontal wind (v) differences from Exp. S for Exps. A, B, and C.

Fig. 7 Derived vertical velocity without using constraints in the objective analysis.

Fig. 8 Derived large-scale temperature tendency without using constraints in the objective analysis

Fig.9 Derived large-scale moisture tendency without using constraints in the objective analysis.

Fig. 10 Derived vertical velocity using the constrained variational analysis.

Fig. 11 Derived large-scale temperature tendency using the constrained variational analysis.

Fig. 12 Derived large-scale moisture tendency using the constrained variational analysis.

Fig. 13 Temperature errors produced by the SCM using the derived large-scale forcing from Exps. S, A, B, and C.

Fig. 14 Moisture errors produced by the SCM using the derived large-scale forcing from Exps. S, A, B, and C.

Table 1. Summary of experiments

Experiments	Brief Description
S	Standard run. T and q are from radiosondes; u and v are from radiosondes merged with wind profiler data; the RUC data are used as background.
A	T and q are from retrievals; u and v are from wind profilers; the RUC data are used as background.
B	Same as A except using the RUC horizontal winds.
C	T, q, u, and v are all from the RUC model.

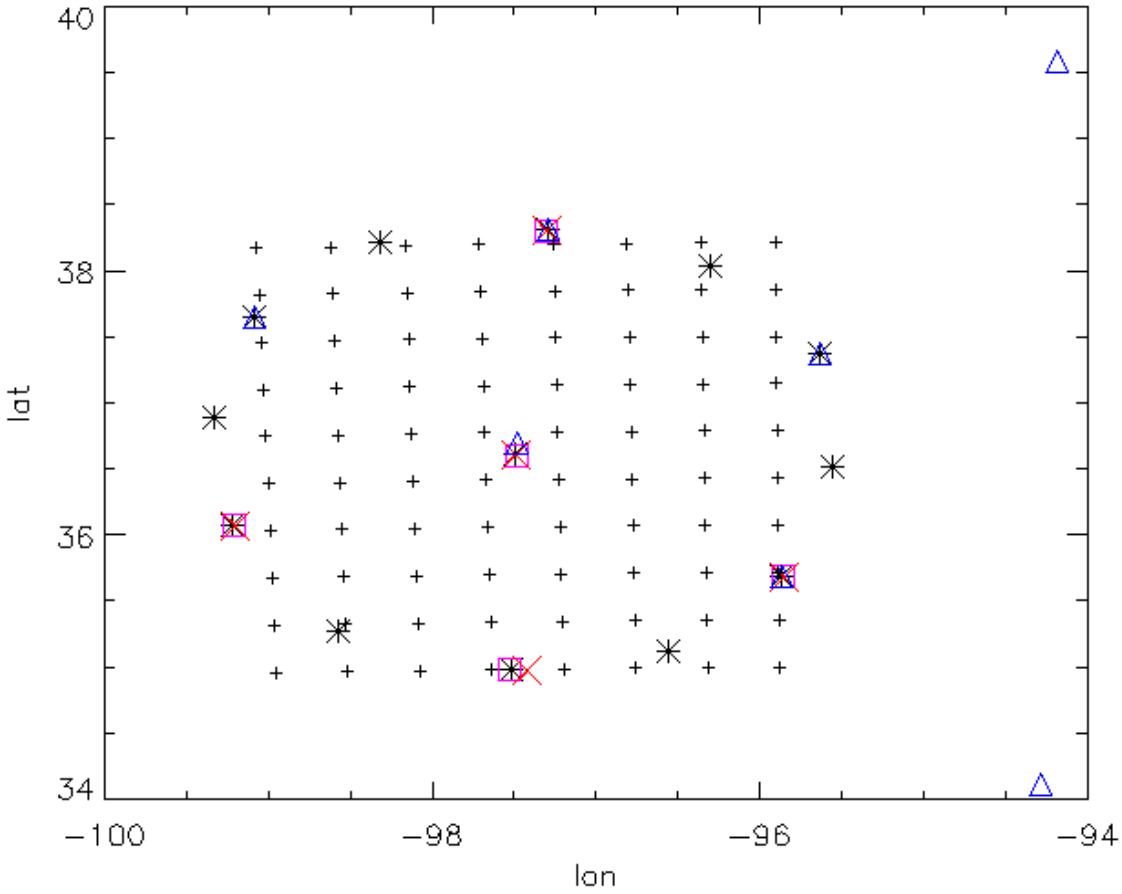

Fig. 1 Locations: Radiosondes (×), AERI (_), NOAA wind profilers (Δ), RUC model grid (+), and final analysis grid (*).

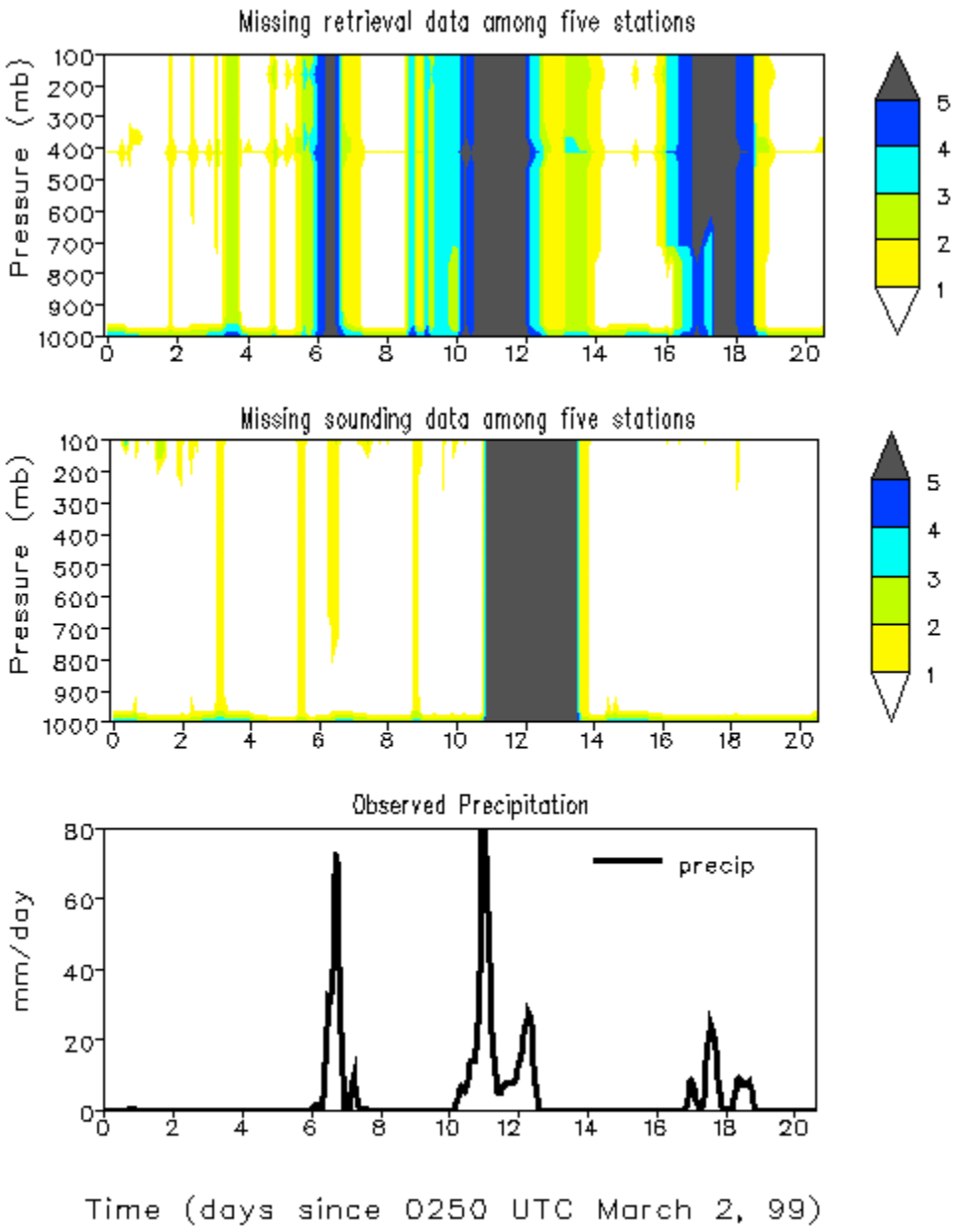

Fig. 2 Missing retrieval and sounding data among the SGP Central Facility and the four SGP Boundary Facilities.

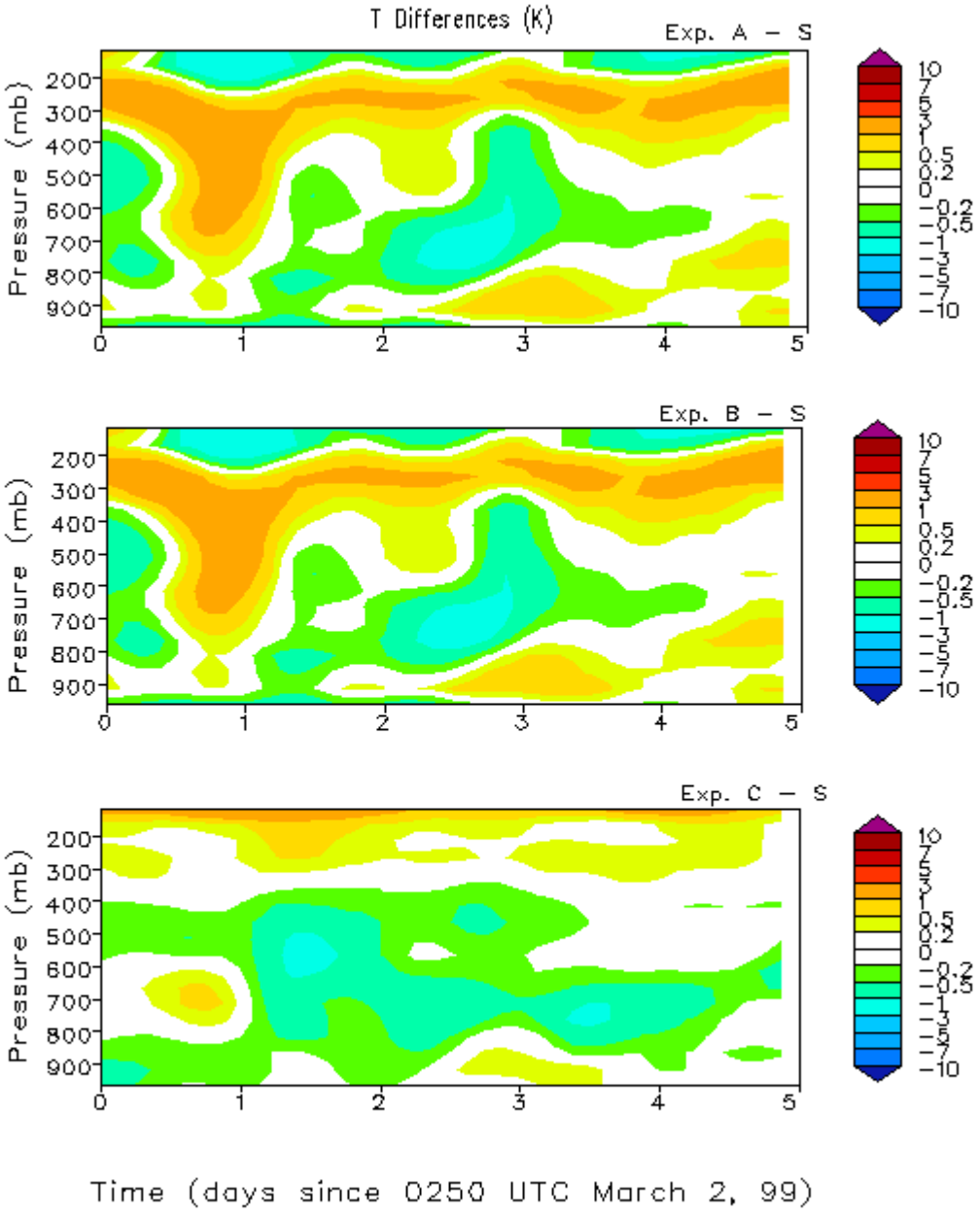

Fig. 3 Temperature differences from Exp. S for Exps. A, B, and C.

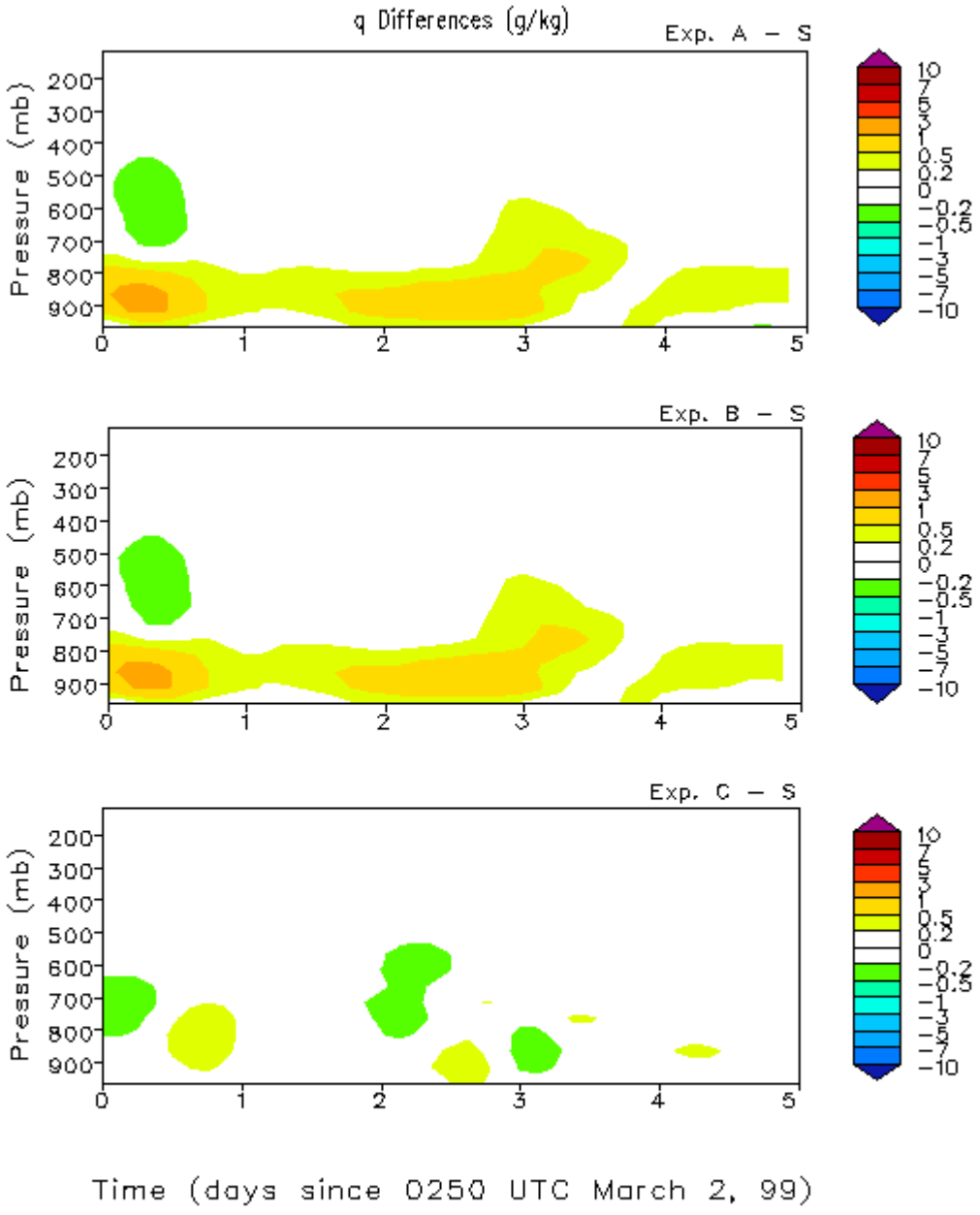

Fig. 4 Moisture differences from Exp. S for Exps. A, B, and C.

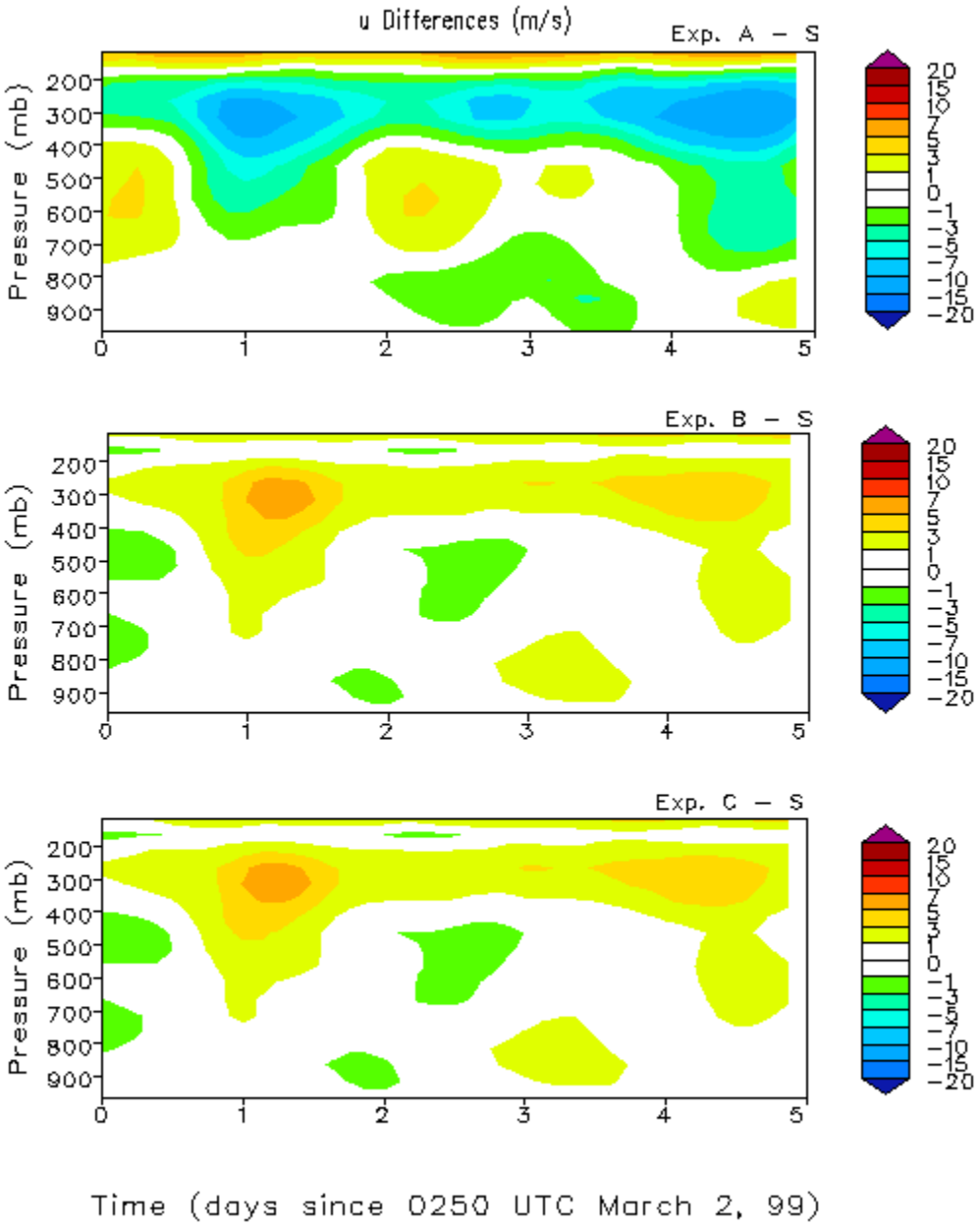

Fig. 5 Horizontal wind (u) differences from Exp. S for Exps. A, B, and C.

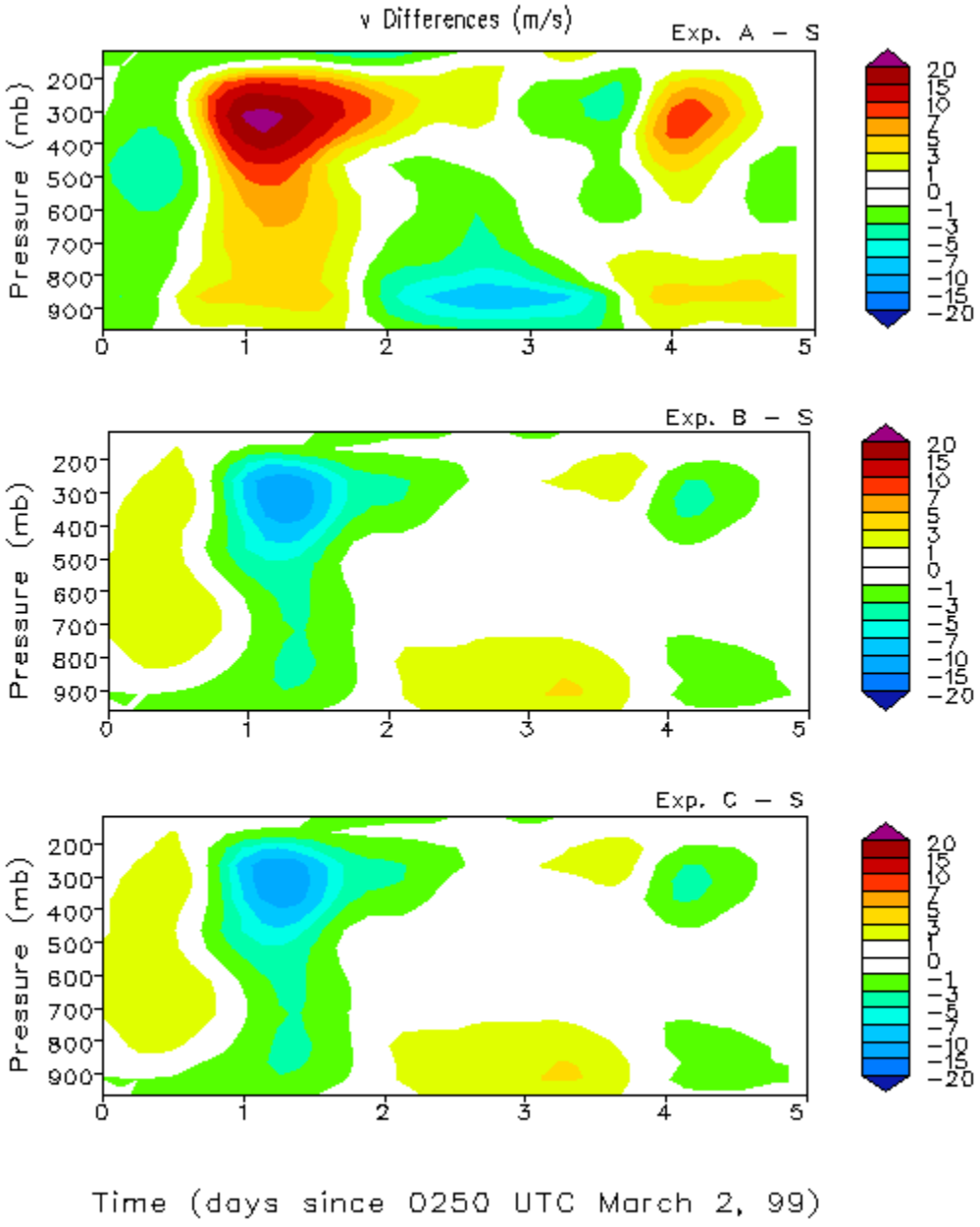

Fig. 6 Horizontal wind (v) differences from Exp. S for Exps. A, B, and C.

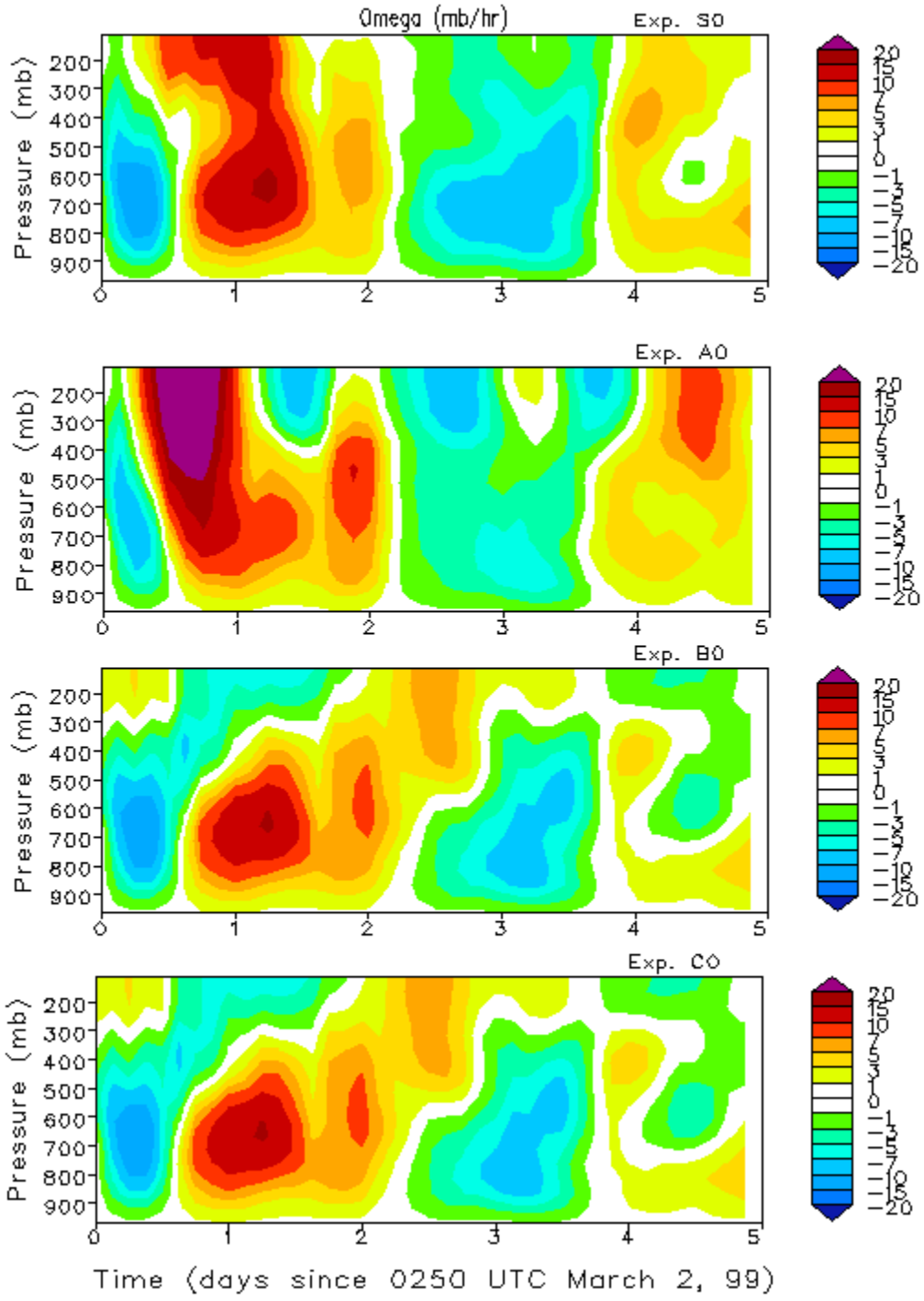

Fig. 7 Derived vertical velocity without using constraints in the objective analysis.

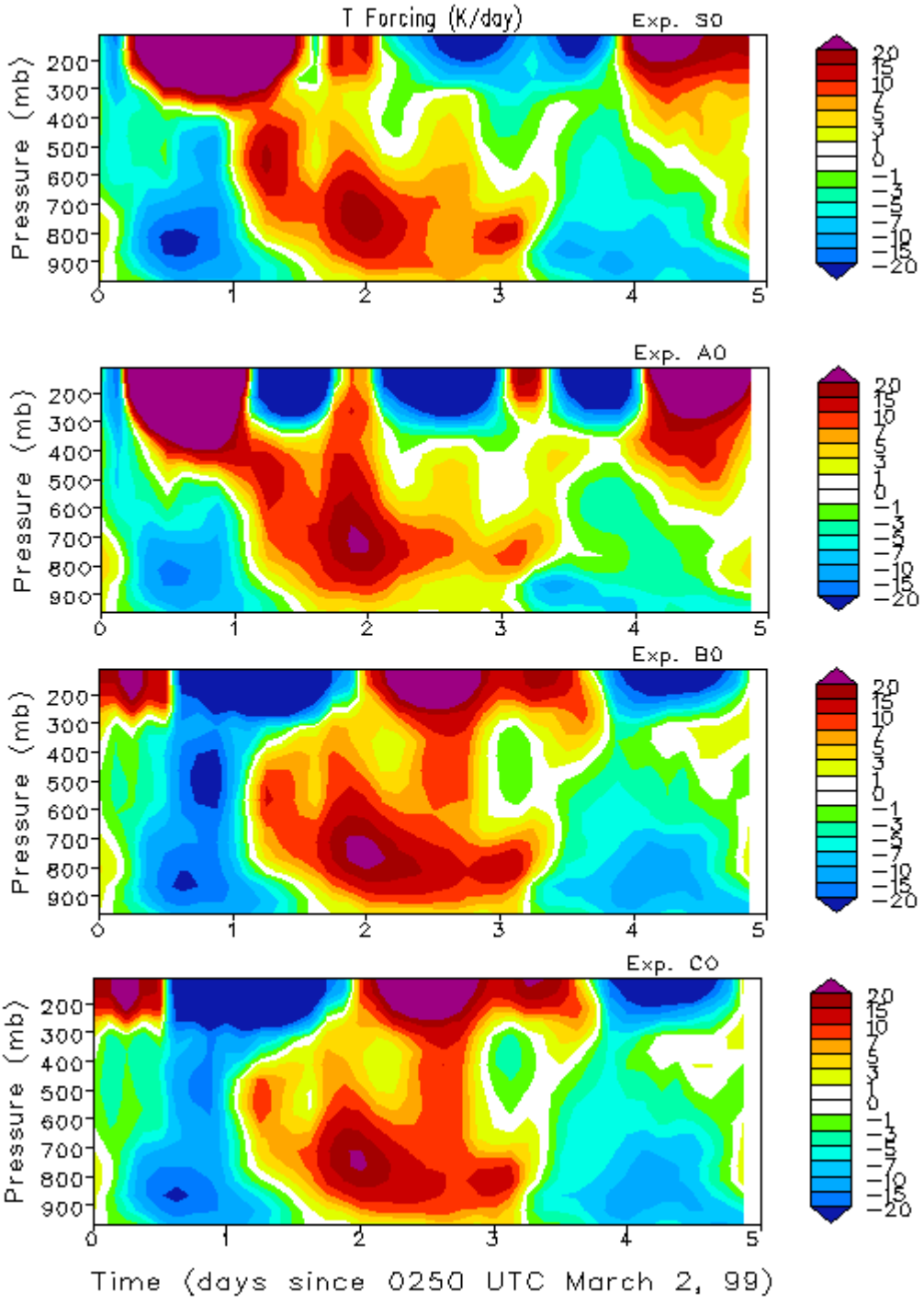

Fig. 8 Derived large-scale temperature tendency without using constraints in the objective analysis

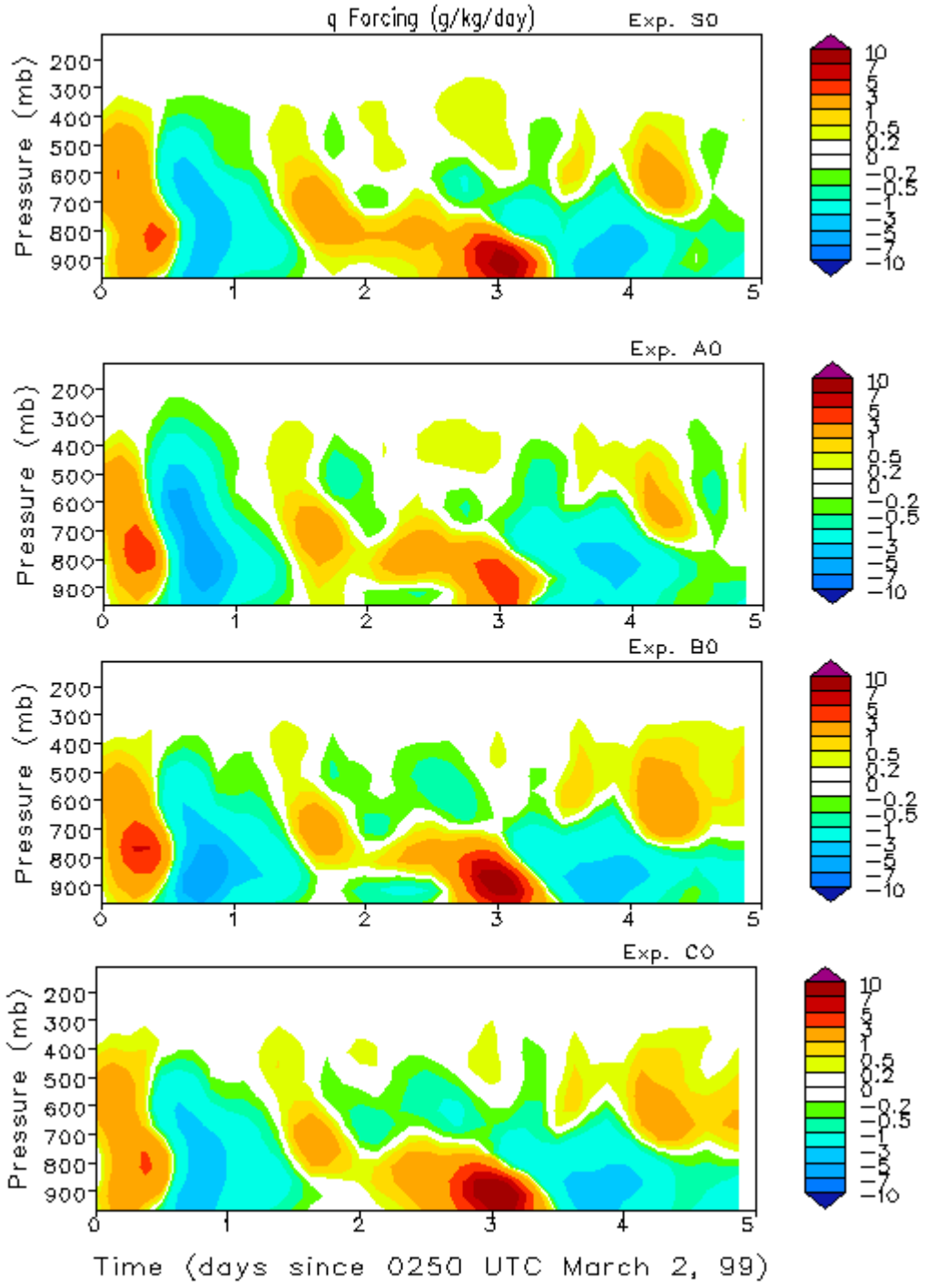

Fig.9 Derived large-scale moisture tendency without using constraints in the objective analysis.

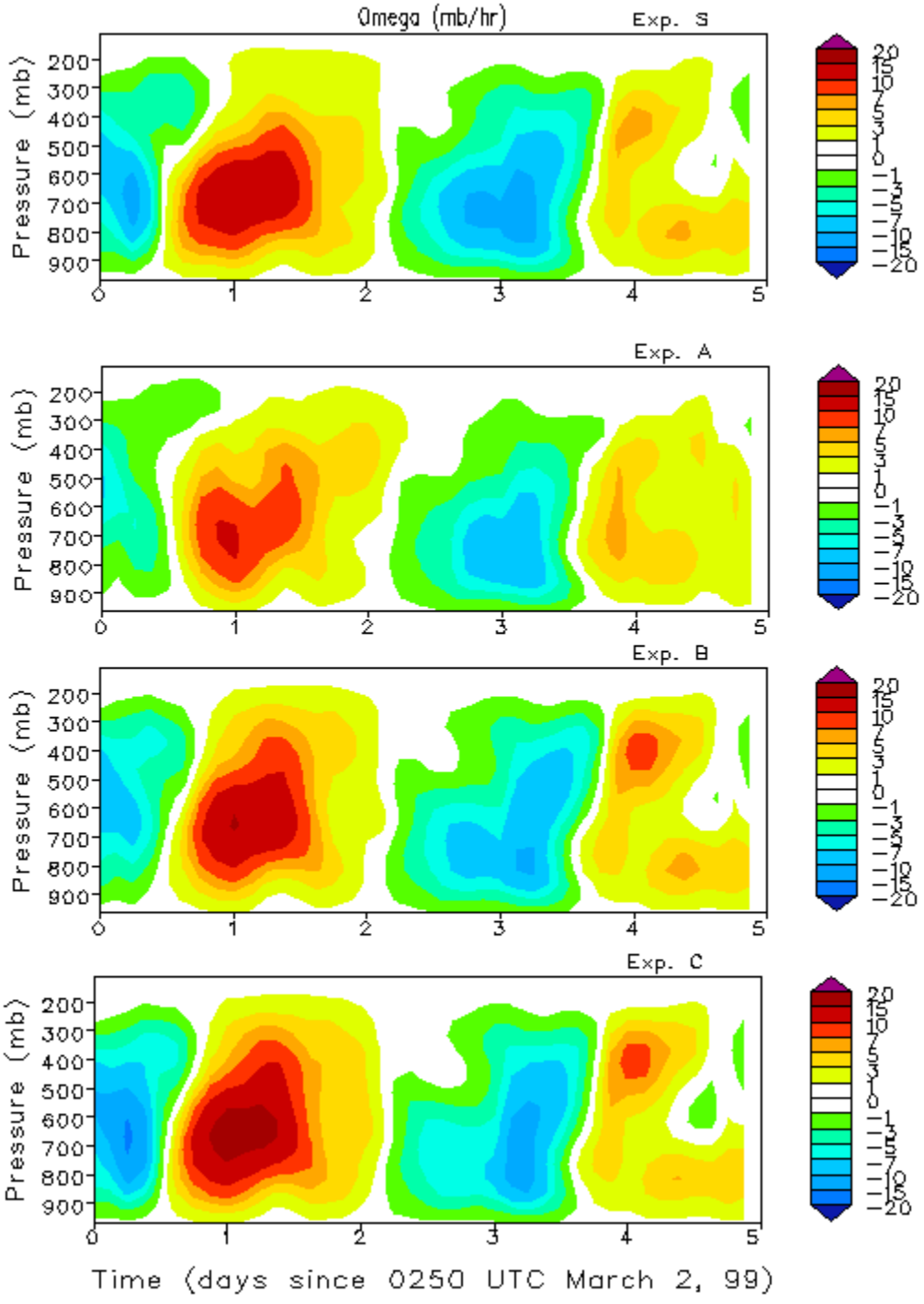

Fig. 10 Derived vertical velocity using the constrained variational analysis.

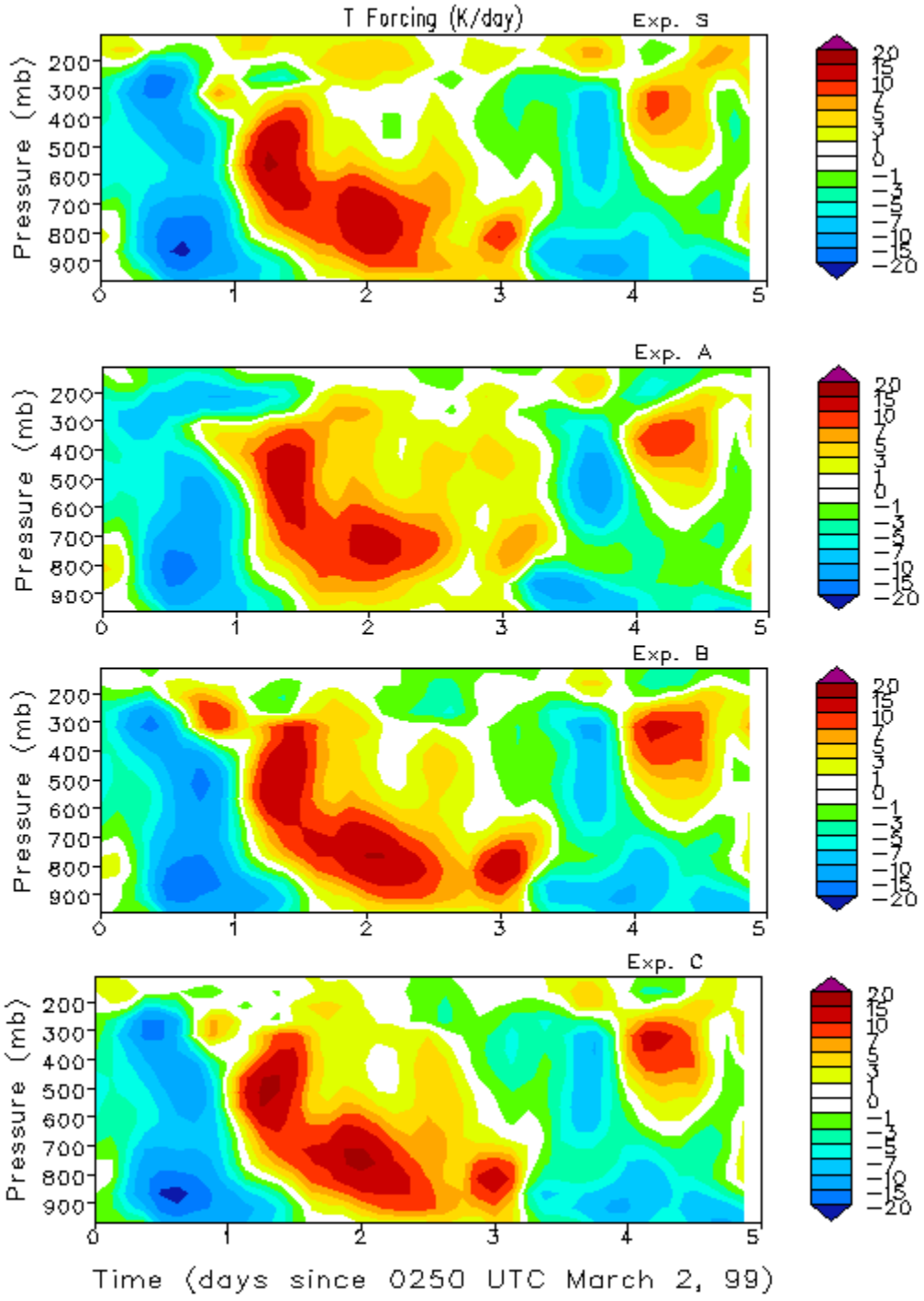

Fig. 11 Derived large-scale temperature tendency using the constrained variational analysis.

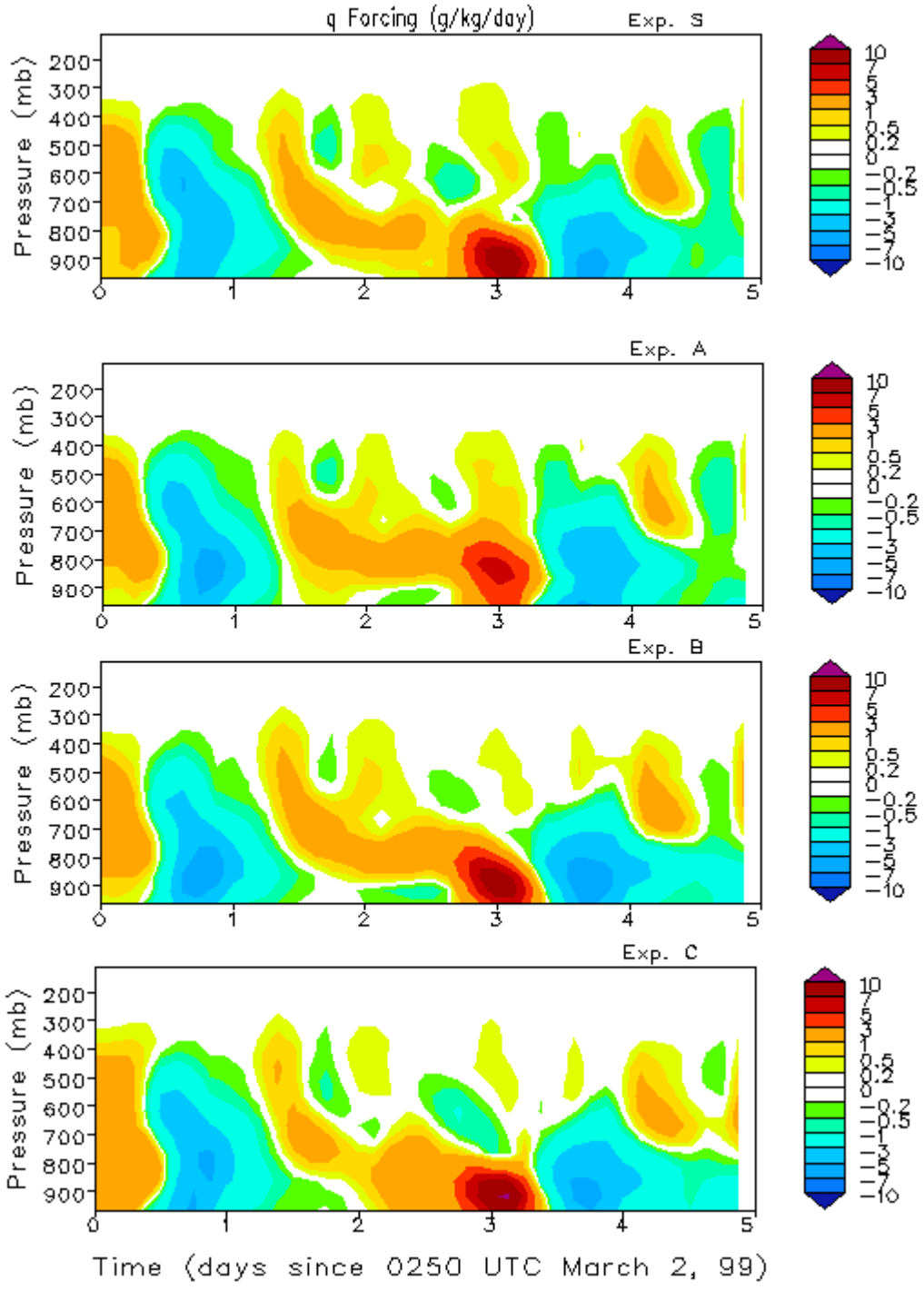

Fig. 12 Derived large-scale moisture tendency using the constrained variational analysis.

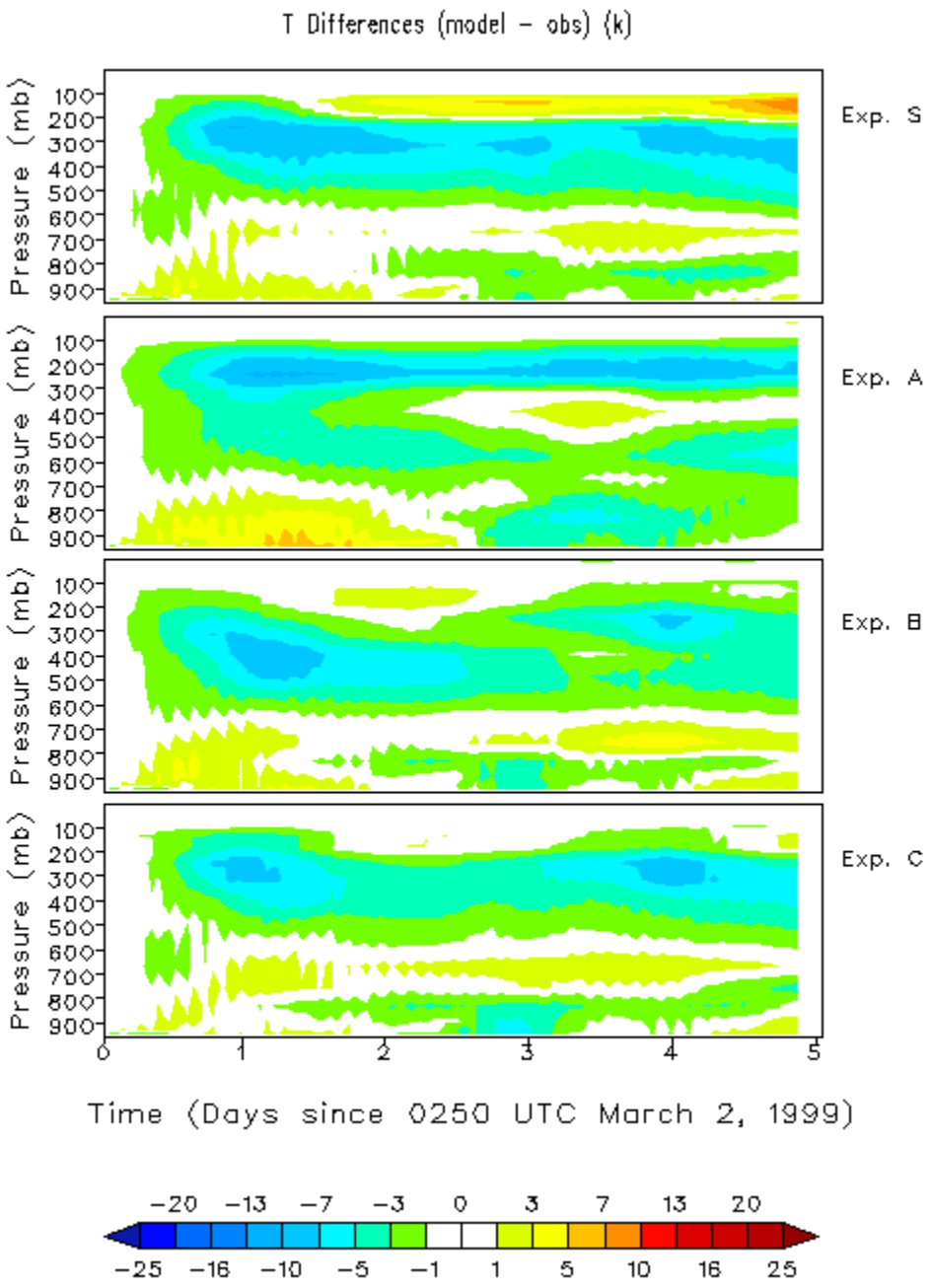

Fig. 13 Temperature errors produced by the SCM using the derived large-scale forcing from Exps. S, A, B, and C.

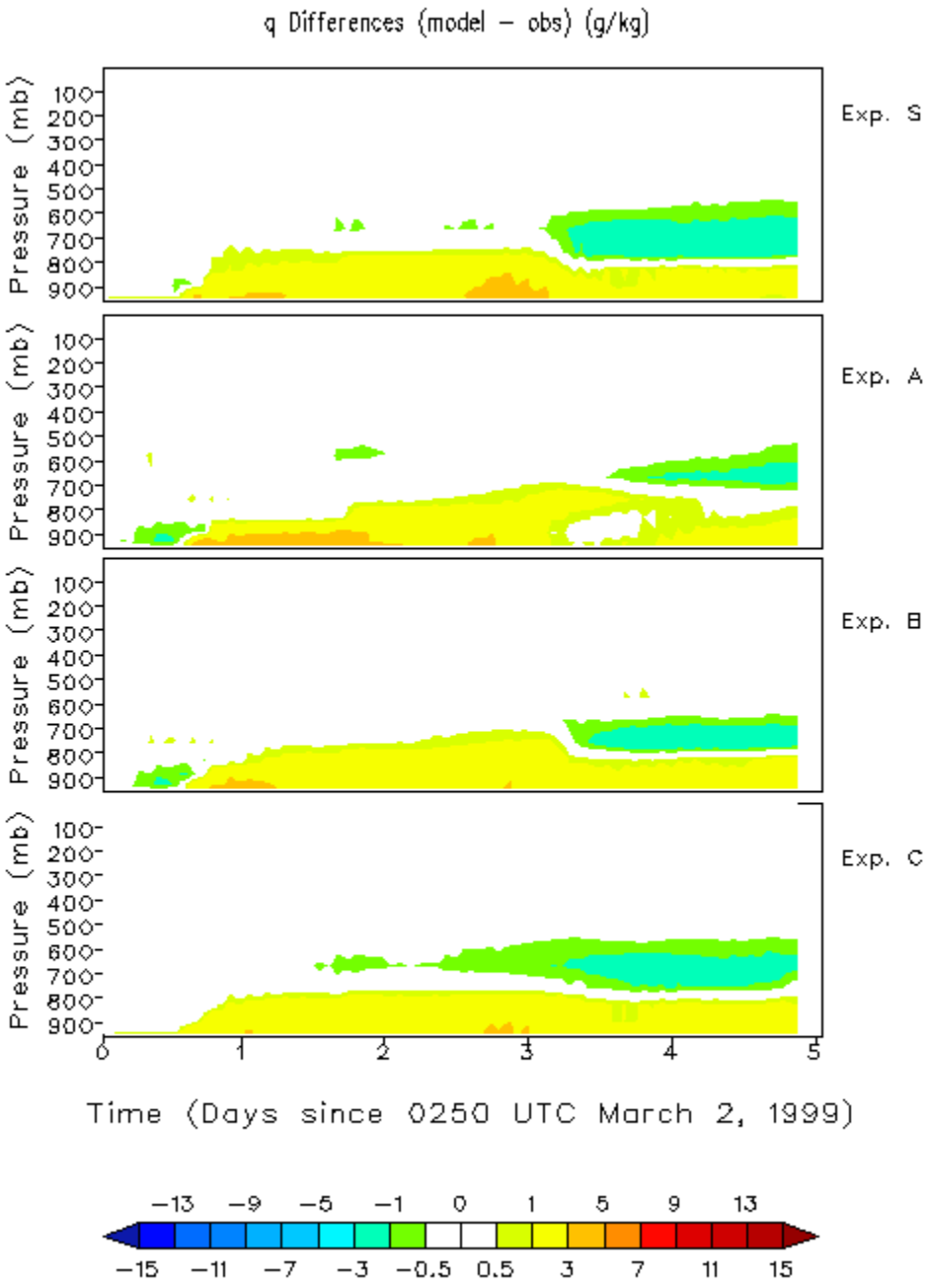

Fig. 14 Moisture errors produced by the SCM using the derived large-scale forcing from Exps. S, A, B, and C.